Received 9 October 2019; revised 21 November 2019; accepted 26 November 2019. Date of publication 2 December 2019;
date of current version 3 January 2020. The review of this article was arranged by Editor C. C. McAndrew.

Digital Object Identifier 10.1109/JEDS.2019.2956981

Analysis and Modeling of Lateral Power Devices With Stepped Drift Region Thickness via Effective Concentration Profile Concept

JUN ZHANG [1,2,3] (Member, IEEE), YU-FENG GUO [1,2] (Member, IEEE), CHEN-YANG HUANG[1,2], AND FANG-REN HU[1,2]

1 College of Electronic Science and Engineering, Nanjing University of Posts and Telecommunications, Nanjing 210003, China
2 National and Local Joint Engineering Laboratory for RF Integration and Micro-Packaging Technologies, Nanjing University of Posts and Telecommunications, Nanjing 210003, China
3 State Key Laboratory of Electronic Thin Films and Integrated Devices, University of Electronic Science and Technology of China, Chengdu 610054, China

CORRESPONDING AUTHOR: Y.-F. GUO (e-mail: yfguo@njupt.edu.cn)

This work was supported in part by the China Post-Doctoral Science Foundation under Grant 2018M642291, in part by the Natural Science Foundation of Jiangsu Province under Grant BK20190237, in part by the National Natural Science Foundation of China under Grant 6190030245, Grant 61574081, and Grant 61704084, and in part by the Opening Project of State Key Laboratory of Electronic Thin Films and Integrated Devices under Grant KFJJ201907.

ABSTRACT Stepped drift region thickness technique alters the drift region doping dose and its distribution, and therefore modulates the device's off-state characteristics. However, due to the sophisticated structure of the 2-D stepped drift region, the conventional 2-D modeling method is too complicated to provide a clear physical meaning. In this paper, based on the Effective Concentration Profile (ECP) theory, a simple but accurate 1-D ECP concept is proposed to unveil the physical insight of the stepped drift region technique and quantitatively analysis the influence of which on device breakdown characteristic. Therefore, the sophisticated 2-D structure affected by both RESURF and curvature effects is explored by a simple 1-D model with segmented-doped PN junction. Furthermore, based on the proposed analytical model, the designing criterion is proposed, which provide useful guidance for utilizing the benefit of the Stepped Drift Region Thickness technique and thus realizing the optimized surface electric field and breakdown voltage. The results obtained by the proposed model are found to be sufficiently accurate comparing with TCAD simulation results.

INDEX TERMS 1-D model, stepped drift region, effective doping, RESURF effect, breakdown voltage.

I. INTRODUCTION

Facing the unceasing demands in simultaneously improving the on- and off-state characteristics, the lateral power devices have developed various techniques to obtain a better trade-off between the breakdown voltage (BV) and specific on-resistance (Ron) [1]–[3]. Since the charge distribution ($Q(x) = N_d(x) \times t_s(x)$) in the drift region plays a decisive role in affecting the performance of lateral power devices, measures such as Variation of Lateral Doping (VLD), Variation of Lateral Thickness (VLT) and Double/Triple-Reduced Surface Field (D/T-RESURF) have been proposed to optimize the surface electric field profile and ultimately obtain the most desirable BV [4]–[8]. Due to the inherent 2-D structure of lateral power device, the optimization of charge distribution can be realized either by altering the doping concentration profile or epitaxial layer thickness. The VLT technique has been proposed to overcome the drawbacks of the VLD such as induced severe local self-heating and on-state characteristic deterioration [6], [8], [9]. Although the VLT technique bypasses the complicated mask layout and long-time/high- temperature annealing of VLD, the epitaxial layer with linear thickness also increases cost and reduces yields. Thus, a more practically accessible VLD technique has been proposed which features a drift region with stepped thickness (ST) [9], [10]. Meanwhile, the irregular structure of the drift region also significantly increases the modeling difficulty of 2-D approaches limiting the utilization of ST lateral power devices in the real world. Especially, due to the abrupt thickness changes between each step, the induced curvature effect may cause strong electric field crowding

near the step edges. Such a sophisticated structure and its 2-D coupling effects make the 2-D model impractical both in explaining the physical nature and in providing design optimization [6], [11], [12].

In this paper, in order to accurately depict the 2-D effect and BV characteristic while providing simple and clear physical insight, we propose the ST-ECP concept which reckons the 2-D coupling and curvature induced crowding effect can be represented by the variation of the ECP in the drift region. Therefore, the inherent 2-D problem is simplified as a 1-D problem reducing the modeling difficulties significantly. Using the proposed method, the ST technique and step-induced curvature effect are thoughtfully explained from the perspective of the ECP. Based on the proposed model, an optimization method is proposed to provide a simple but efficient designing guidance. The analytical model is validated by the good agreement between the modeling results and simulation results by MEDICI, technology computer-aided design (TCAD) tool. The simulation models used in MEDICI are CONSRH, AUGER, BGN, FLDMOB, IMPACT.I and CCSMOB.

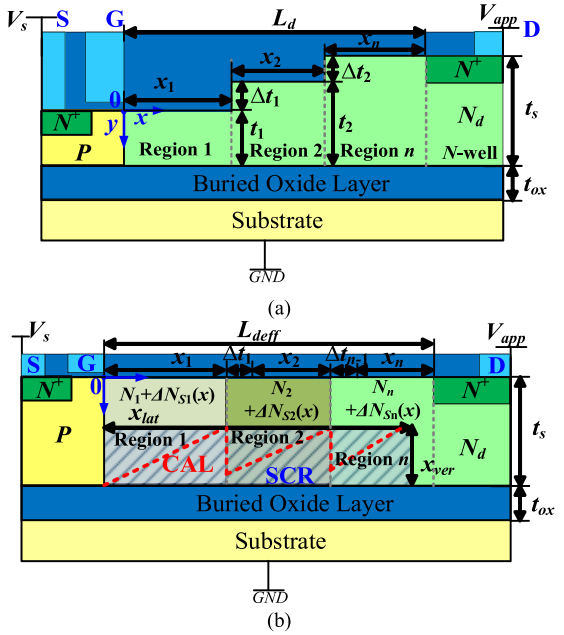

FIGURE 1. (a) 2-D cross section of the SOI LDMOS with stepped drift region and (b) the ECP equivalent structure for modeling (*x*-*y* plane).

II. EFFECTIVE CONCENTRATION PROFILE

The effective concentration profile serves as a bridge that connects the simple 1-D equivalent structure and sophisticated 2-D devices and therefore plays a core role in the 1-D ST-ECP model. Specifically, as shown in Fig. 1 (a), a 2-D cross-section of the lateral power devices with stepped drift region thickness is applied to quantitatively determine the ECP in the drift region. For region i, the drift region thickness is t_i while t_s is the epitaxial layer thickness. When a reverse-biased voltage is applied, the 2-D coupling effect and curvature effect near the step simultaneously act on its breakdown characteristics. In which case, in order to derive an analytical model using conventional 2-D modeling methods, the modified Bessel function has to be applied making the mathematic expression too complicated to explore the physical insight of these effects and its coupling effect [6], [11]. Whereas, since the ECP concept assumes that the inherent 2-D effects can be equivalent by the variation of the effective concentration in the drift region [4]. Therefore, the dimensionality reduction of the problem from 2-D to 1-D can be realized. For the ST device shown in Fig. 1 (a), the stepped drift region thickness, 2-D RESURF effect, and curvature effect induced by the abrupt step both lay its influence on ECP. Thus, the effective concentration profile ($N_{eff}(x)$) can be easily obtained by using the principle of compensation semiconductor, which yields:

$$N_{eff}(x) = N_d + \Delta N_{eff-RESURF} + \Delta N_{eff-ST} + \Delta N_S \quad (1)$$

where N_d being the actual doping concentration of the drift region, ΔN_{eff-ST}, $\Delta N_{eff-RESURF}$, and ΔN_S represent the increment of ECP as a result of stepped drift region thickness, RESURF effect, and curvature effect, respectively. In order to quantitatively obtain N_{eff}, the influence of those effects on the device's off-state characteristic can be separately analyzed.

The doping dose of the drift region has a significant influence on the device's BV characteristic. Both the VLD and VLT techniques optimize the device off-state performance relies on this principle. For an ST lateral power device, the doping dose of region i satisfies $Q_i = N_d \times t_i$. In order to reduce the dimensionality, the doping dose of region i can be re-written as $Q_i = N_i \times t_s$. Accordingly, $N_i = N_d \times t_i/t_s$ being the equivalent doping concentration of region i. Thus, as shown in Fig. 1 (b), the actual device with stepped drift region thickness can be equivalent to a lateral power device with Step Doping Profile(SDP). Therefore, the effect of effective doping concentration N_i and 2-D coupling effect on ECP ought to be in accordant with that in [12], which yields:

$$N_{eff}(x) = N_i + \Delta N_{eff-RESURF} + \Delta N_{Si}, L_{i-1} < x \le L_i \quad (2)$$

where $\Delta N_{eff-RESURF} = -\eta x N_d / Min[x_{lat}, L_{eff}]$ indicates the influence of the 2-D coupling effect on ECP [4]. Unlike that in the SDP device, due to the existence of the steps, the drift region surface length of the ST device is equivalently extended. In which case, the effective drift region length satisfies $L_{deff} = L_d + \Delta t_d$. Therefore, the effective boundary of region i is determined by $L_i = x_1 + x_2 + \cdots + x_i + (t_i - t_1)$ and $L_{i-1} = x_1 + x_2 + \cdots + x_{i-1} + (t_{i-1} - t_1)$. The $\Delta t_d = t_s - t_1$ represents the overall thickness variation of the drift region. Accordingly, the effective surface length of region i ought to satisfy $x_{eff\_i} = x_i + \Delta t_{i-1}$. Apparently, the Δt_0 is zero. L_d is the physical length of the drift region. In this paper, $\eta = x_{ver}(V_{app})/t_s$ is the ratio of vertical depletion length at $x = Min[x_{lat}, L_{deff}]$ and SOI layer thickness. The

η is applied to describe the 2-D coupling between vertical and lateral structure. According to [4] and [12], the Charge Appointment Line in ST device also satisfies $\mathrm{CAL}(x) = \eta x N_d / Min[x_{lat}, L_{deff}]$.

However, unlike the case of SDP lateral power devices, the ST structure introduces curvature induced electric field crowding near the step between each region. Such a crowding effect may sabotage the designed electric field profile dramatically reducing the BV. Meanwhile, the prediction and optimization of step-induced curvature effect are infeasible as its very much difficulty in modeling using conventional approaches. In order to bypass the complicated 2-D approaches, a 1-D method is proposed to predict and analyze the step-induced curvature effect. For a single-side 1-D polar junction, the ECP increment as a result of the abrupt step can be easily obtained by directly solving 1-D Poisson's equation in the polar coordinate system, which yields [4]:

$$N_{Polar}(x) = N_d + \Delta N_{Polar}(x) = N_d\left(1 - \frac{L_j^2}{x^2}\right) \tag{3}$$

where L_j is the junction radius at $x = L_j$. As shown in Fig. 1 (a), for the regions that have steps at both ends of the region boundaries, the step-induced curvature effect is more complicated [8], [9], [13]. In this case, the ECP is affected by the curvature effect at both ends simultaneously. Thus, considering the effective concentration differences between regions, we propose that the increment in a result of step-induced curvature effect of right and left sides of region i can be respectively given as:

$$\Delta N_{Step\_right}(x) = -\frac{(N_i - N_{i-1})\Delta t_i^2}{(L_i + \Delta t_i - x)^2},\ L_{i-1} < x \le L_i \tag{4}$$

$$\Delta N_{Step\_Left}(x) = \frac{(N_{i-1} - N_{i-2})\Delta t_{i-1}^2}{(x - L_{i-1} + \Delta t_{i-1})^2},\ L_{i-1} < x \le L_i \tag{5}$$

The Eq. (4) and (5) can be further simplified by using $N_i = N_d \times t_i / t_s$. Therefore, for the regions that have step-induced curvature effect in both ends, the overall ECP increment of step-induced curvature effect upon region i can be obtained using Eq. (4) and (5), which yields:

$$\Delta N_{Si}(x) = \frac{N_d}{t_s}\left[\frac{\Delta t_{i-1}^3}{(x - L_{i-1} + \Delta t_{i-1})^2} - \frac{\Delta t_i^3}{(L_i + \Delta t_i - x)^2}\right],\quad 1 < i < n \tag{6}$$

The proposed method reckon the step as a ring-like so that the simple polar coordinate system can be used to predict the influence of step-induced electric field crowding. In fact, such a method is not mathematically rigorous since the actual step is a right angle region. Nevertheless, the proposed method is proven to be accurate and effective in depicting and predicting the step-induced electric field crowding by good agreements between simulations and analytical results. So far, the rather complicated 2-D structure and its coupling effects have converted to the variation of lateral ECP. Thus, the surface electric field and lateral BV characteristic can be depicted simply via solving 1-D Poisson's equation directly, which yields:

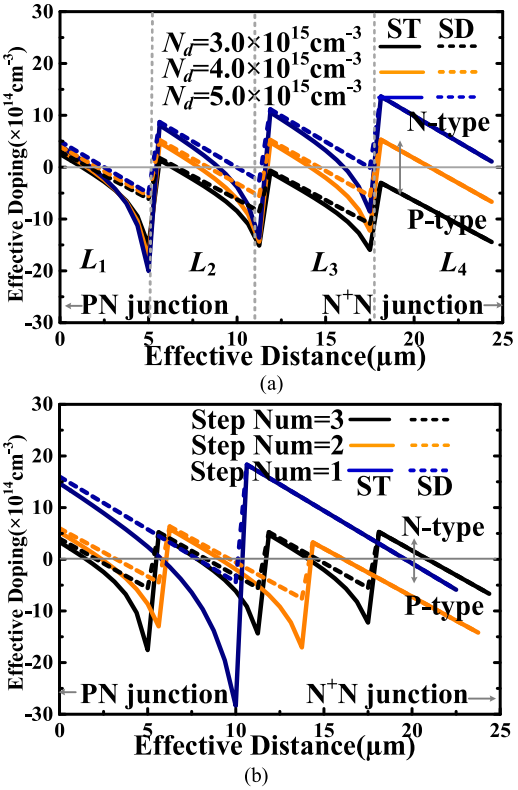

FIGURE 2. Effective Doping Concentration of the drift region for various (a) drift region doping concentration (V_{app} = 250V, $x_1 = x_2 = x_3 = x_4 = 5\mu m$, $t_1 = 0.5\mu m$, $t_2 = 2\mu m$, $t_3 = 3.5\mu m$, $t_s = t_4 = 5\mu m$), (b) Step numbers ($N_d = 3.0 \times 10^{15} cm^{-3}$, S1: $x_1 = x_2 = 10\mu m$, $t_1 = 2\mu m$, $t_2 = 5\mu m$; S2: $x_1 = x_2 = 6\mu m$, $x_3 = 8\mu m$, $t_1 = 1\mu m$, $t_2 = 3\mu m$, $t_3 = 5\mu m$) with $t_s = 5\mu m$, $t_{ox} = 2\mu m$, $L_d = 20\mu m$.

$$\frac{d^2\varphi(x,0)}{dx^2} = \frac{dE(x,0)}{dx} = -\frac{qN_{eff}(x)}{\varepsilon_s} \tag{7}$$

Fig. 2 intuitively shows the influence of stepped drift region and step-induced curvature effect on ECP in comparison with lateral power device using Step Doping(SD) profile. As shown in Fig. 2 and 3, the periodically-appearing equivalent NP structures in drift region create electric field valley and peaks. Although the SD and ST technique both reshape the surface electric field and lateral BV characteristic by altering the drift region doping dose, the ST method has a more complicated ECP due to the step-induced curvature effect. In fact, the curvature effect near the right corner of each region may take the leading position in affecting ECP. The curvature effect near the step leads to a rapid ECP drop indicating a sharp electric field peak is expected near the step. In which case, as shown in Fig. 2 (a), the doping concentration of drift region itself has a minor effect on the ECP at this very position indicating the drift region doping concentration can be boost significantly to achieve a better on-state characteristic. Hence, the severe local self-heating and on-state characteristic deterioration caused by low doping concentration near the PN junction in VLD lateral power

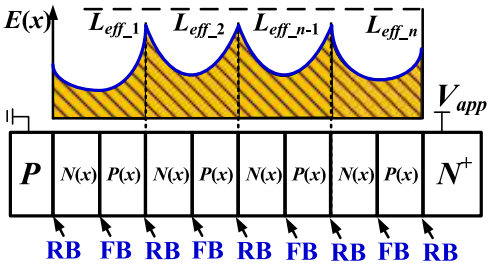

FIGURE 3. Effective lateral structure and the electric field distribution of the drift region with Stepped Thickness. (RB: Reverse-Biased, FB: Forward-Biased).

devices can be avoided. Moreover, as Fig. 2 (b) indicates, the step number also has a decisive influence on the drift region's ECP. A small number of steps means a big step drop between regions causing a more severe electric field crowding effect near the step and thus resulting in a sharper ECP change. Obviously, a more ideal surface electric field profile and lateral BV characteristic can be achieved by setting more and shorter steps in the drift region. When the step number tends to infinity, the ST method is converted to the VLD technique, the ideal even surface electric field profile is obtained with the linear thickness of drift region. Nevertheless, as mentioned above, such solution inevitably adds process steps and fabrication complexity, therefore, increases cost and reduces yields.

III. SURFACE ELECTRIC FIELD

A. SURFACE ELECTRIC FIELD PROFILE

As Eq. (2) indicates, the effect of drift region doping adjustment, 2-D RESURF effect, and curvature effect induced by the abrupt step can be equivalent to independent ECP increments. Hence, according to the 1-D Poisson's equation, the surface electric field profile can be easily obtained by adding up the EF increment of those effects, which yields:

$$E_i(x) = E_{i-1} + \Delta E_{STi}(x) + \Delta E_{RESURF}(x) + \Delta E_{Si}(x) \tag{8}$$

$$\Delta E_{STi}(x) = -\frac{qN_i}{\varepsilon_s}x \tag{9}$$

$$\Delta E_{RESURF}(x) = \frac{qN_d}{2\varepsilon_s}\cdot\frac{\eta x^2}{Min[x_{lat}, L_d]} \tag{10}$$

$$\Delta E_{Si}(x) = \frac{qN_d}{\varepsilon_s t_s}\left[\frac{\Delta t_{i-1}^3}{(x - L_{i-1} + \Delta t_{i-1})} + \frac{\Delta t_i^3}{(L_i + \Delta t_i - x)}\right] \tag{11}$$

where E_{i-1} is obtained by using $E_{i-1}(L_{i-2}) = E_{i-2}(L_{i-2})$. To further verify the veracity of the proposed model and illustrate the influence of ST structure on lateral off-state characteristics, we have compared the modeled surface EF with TCAD results as shown in Fig. 4 (a) and (b). The consistency between the analytical results and the simulations has demonstrated the correctness of the proposed 1-D model. The combined impact of ST structure and step-induced curvature

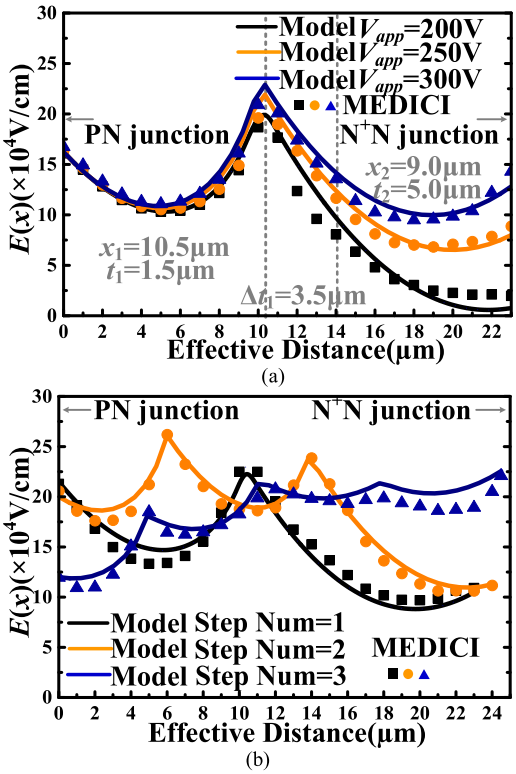

FIGURE 4. Analytical and numerical surface electric field profiles of the drift region for various (a) Applied Voltage ($N_d = 3.0 \times 10^{15}\text{cm}^{-3}$), (b) Step numbers ($V_{app} = 300\text{V}$, $N_d = 4.0 \times 10^{15}\text{cm}^{-3}$, S1: $x_1 = x_2 = 10\mu\text{m}$, $t_1 = 2\mu\text{m}$, $t_2 = 5\mu\text{m}$; S2: $x_1 = x_2 = 6\mu\text{m}$, $x_3 = 8\mu\text{m}$, $t_1 = 1\mu\text{m}$, $t_2 = 3\mu\text{m}$, $t_3 = 5\mu\text{m}$) with $t_s = 5\mu\text{m}$, $t_{ox} = 2\mu\text{m}$, $L_d = 20\mu\text{m}$.

effect has a sophisticated result on lateral BV characteristic. As shown in Fig. 4 (a), the electric field varies little within the step-affected regions due to the strong influence of the curvature effect near its right end. However, as Fig. 2 and 4 indicate, region n only weakly affected by the curvature effect from its left end and therefore the surface EF in region n is a strong function of the applied voltage. Moreover, even the more step number of the drift region will not necessarily ensure a better surface electric field profile. As Fig. 4 (b) indicates, the poorly designed structure parameters promote the crowding near the steps causing the high surface electric field peaks. Obviously, such the complicated coupling effect of ST devices significantly complex the optimization process of structure parameters.

B. SURFACE ELECTRIC FIELD OPTIMIZATION

To maximum the breakdown characteristic of the lateral structure, it is desirable to even the surface electric field. For the lateral power device with stepped drift region thickness, the period-appears valleys and peaks are inevitable. Therefore, in which case, the best scenario is all peaks of the surface electric field reach the critical electric field (E_C) simultaneously, namely:

$$E(x_i, 0) = E(x_{i+1}, 0) = E(x_{i-1}, 0) = E_C \tag{12}$$

Considering the fact that the drift region in a practical lateral power device is already fully depleted when the breakdown occurs so that a good off-state characteristic can be achieved, the optimization of the surface electric field in this paper is premised on the full depletion condition. Therefore, by submitting Eq. (12) into (8), the geometric optimization criterion to achieve the optimized surface electric field can be obtained, which yields:

$$\frac{\eta t_s}{2L_d}\left(L_i^2 - L_{i-1}^2\right) - t_i(L_i - L_{i-1}) + \left(\frac{\Delta t_{i-1}^3}{\Delta t_{i-1} + L_i - L_{i-1}} - \frac{\Delta t_i^3}{\Delta t_i + L_i - L_{i-1}}\right) = 0 \quad (13)$$

Although the direct solving of Eq. (13) is complicated and cumbersome, the using of a particular solution can significantly simplify the solving process. As Eq. (13) indicates, the step-induced curvature effect at left and right end of each region can be neutralized when $\Delta t_i = \Delta t_{i-1} = \Delta t_{i+1}$. Therefore, the geometric optimization criterion can be further simplified by using $t_i = i/n \times t_s = i \times \Delta t$, which yields:

$$\frac{(L_i + L_{i-1})}{L_d} \cdot \frac{\eta}{2} = \frac{i}{n} \quad (14)$$

The curvature effect in region 1 and n only have a step at one end making the neutralization of the curvature effect impossible. However, in practice the region length usually satisfied $L_1 >> \Delta t$ and $L_n + L_{n-1} >> \Delta t$ making the Eq. (14) still feasible in optimizing the surface electric field of region 1 and n. The optimized coupling factor η_{opt} can be further obtained using $L_n = L_{deff}$ and Eq. (14), which yields:

$$\eta_{opt} = \frac{2L_n}{(L_n + L_{n-1})} \quad (15)$$

Eq. (15) indicates that the optimized η is a strong function of region/step number. When $n = 1$, the ST case degenerates to S-RESURF case and the ideal η equals to 2. Meanwhile, when the step number tends to infinity, the ST structure becomes VLT structure, in which case the ideal η equals to 1 meaning the drift region just fully depleted when the lateral breakdown happens. Such conclusions are also fit the lateral breakdown theory presented in [4] and [12], respectively. Therefore, by submitting Eq. (15) into (14), the actual length of each region (Δx_i) can be further obtained which ought to satisfies $\Delta x_i = \Delta x = L_d/n$. Namely, the effective length of each region is $\Delta L = \Delta x + \Delta t$.

So far, with the usage of optimized drift region structure ($\Delta x_i = L_d/n = \Delta x$, $t_i = i/n \times t_s = i \times \Delta t$), the step-induced curvature effect in each region is neutralized by using the mutual compensation between the electric field crowding effect near the left and right corner. Fig. 5 intuitively shows the optimized surface electric field profile after applying the geometric optimization criterion. The discrepancies between the analytical results and simulations at NN^+ junction is reckoned as the outcome of the electric field crowding caused by the shallow drain active region. As shown in Fig. 5 (a),

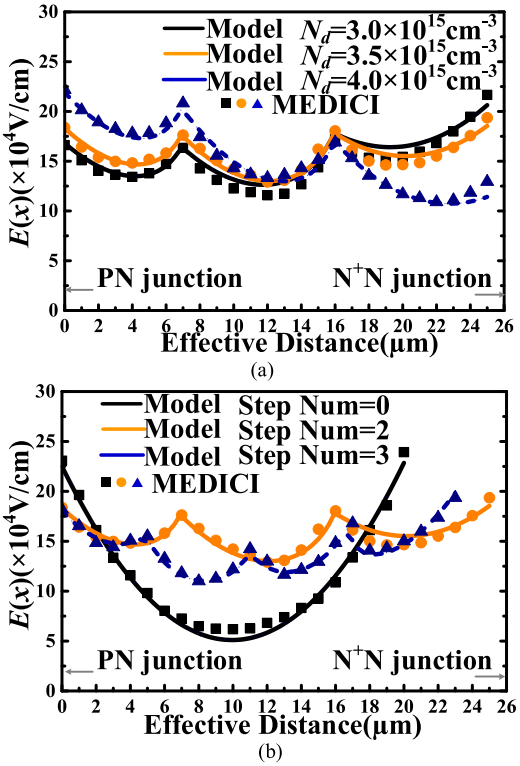

FIGURE 5. Analytical and numerical surface electric field profiles using the geometric optimization criterion for various (a) Drift region doping (S2: V_{app} = 300V, L_d = 21μm, t_s = 6μm) and (b) Step number (S0: V_{app} = 250V, N_d = 2.5 × 10^{15}cm^{-3}; L_d = 20μm, t_s = 5μm; S2: V_{app} = 300V, N_d = 3.5 × 10^{15}cm^{-3}; L_d = 21μm, t_s = 6μm; S3: V_{app} = 300V, N_d = 5.0 × 10^{15}cm^{-3}; L_d = 20μm, t_s = 4μm) with t_{ox} = 2μm.

even applied the geometric optimization criterion, the surface EF profile is very still sensitive to the drift region doping concentration, the under- or over-estimation of η will sabotage the optimized surface EF causing the deterioration of lateral BV characteristic. For the ST device already with the optimized surface EF, its lateral BV characteristic is mainly a function of step numbers. As Fig. 5 (b) shows, more step numbers indicate a smaller difference between the EF peaks and valleys bringing a lower maximum surface EF peak. Although more step number enables a better lateral BV and higher N_d, it also causes more process steps which ultimately adds costs and reduces yields. Therefore, the vertical structure and its BV characteristic also ought to be considered in order to take benefits from the interaction between the lateral and vertical breakdown.

IV. BREAKDOWN VOLTAGE

The off-state characteristic of a lateral power device is determined by the weakest one in BV between the lateral and vertical structures. For the lateral structure in accordance with the geometric optimization criterion defined by Eq. (14), its breakdown voltage can be obtained by submitting Eq. (8) and (14) into 1-D Poisson's equation, which yields:

$$BV_{lat} = E_{n-1}L_{eff} + V_{ST} + V_{RESURF} + V_S \quad (16)$$

$$V_{ST} = -\frac{q}{\varepsilon_s}\sum_{i=1}^{n} N_i\left(L_i^2 - L_{i-1}^2\right) \tag{17}$$

$$V_{RESURF} = \frac{qN_d L_{eff}^2 \eta}{6\varepsilon_s} \tag{18}$$

$$V_S = -\frac{qN_d \Delta t^3}{\varepsilon_s t_s} \ln\left(\frac{\Delta L^2 + \Delta t \Delta L}{\Delta t^2}\right) \tag{19}$$

where the E_{n-1} satisfies $E_{n-1} = E_0 + 0.5qN_dL_{n-1}/\varepsilon_s(\eta L_{n-1}/L_n - 1)$. In this paper, the critical electric field (E_C) is determined by $E_C = 3.0 \times 10^5/[1 - 0.33\log_{10}(N_d/10^{16})]$(V/cm) [4], [5], [12]. The Eq. (19) indicates that the BV falling induced by electric field crowding is a strong function of step number. When n tends to infinity, both the ΔL and Δt tends to zero, therefore, the V_s tends to zero. In which case, the Eq. (16) is consistent with BV expression in SDP cases. As shown in Fig. 5 (a), the lateral breakdown may occur at the PN or NN^+ junction as a result of the over- or under-estimation of drift region depletion, respectively. For the NN^+ junction breakdown, the actual depletion in drift region excesses the optimized 2-D coupling factor ($\eta > \eta_{opt} \geq 1$) causing the elevation of electric field peak at NN^+ junction. In which case, full-depletion NN^+ breakdown (FNN) occurs. On the contrary, when $\eta < \eta_{opt}$ and $\eta \geq 1$, the lateral full-depletion PN breakdown (FPN) occurs with the surface electric field reaches its maximum at the PN junction. In particular, for the partial-depletion case, the $\eta < 1$ and the partial-depletion PN breakdown (PPN) occurs. Obviously, as shown in Fig. 6, such case ought to be avoided during the designing phase for its low breakdown voltage and area utilization rate [12]. As for the vertical structure, the vertical breakdown only occurs under the full-depletion condition. Thus, its breakdown voltage can be obtained by:

$$BV_{ver-F} = \frac{qN_d t_s}{\varepsilon_s}\left(K\eta t_{ox} + \frac{2\eta - 1}{2} t_s\right) \tag{20}$$

In practice, if the epitaxial layer is not thick enough to ignore the depth of the N^+ diffusion region (t_j), the effective thickness of the SOI layer for the vertical breakdown should be $t_{se} = t_s - t_j$ [12]. In fact, in order to maintain a high BV while achieving a big process tolerance, it is desirable to make device happens vertical breakdown other than lateral breakdown which is very sensitive to the device parameters.

As discussed earlier, the overall breakdown voltage of the ST lateral power device is determined by the lowest among lateral and vertical breakdown voltage, which yields:

$$BV = Min[BV_{lat}, BV_{ver}] \tag{21}$$

Same as that in S-RESURF case, the breakdown of ST lateral power devices may successively undergo NN^+ junction full-depletion, vertical breakdown, PN_d junction full depletion, and PN_d junction partial-depletion with the increase of N_d. As that in ST devices, the region/step number plays a decisive role in affecting the lateral BV characteristic. As

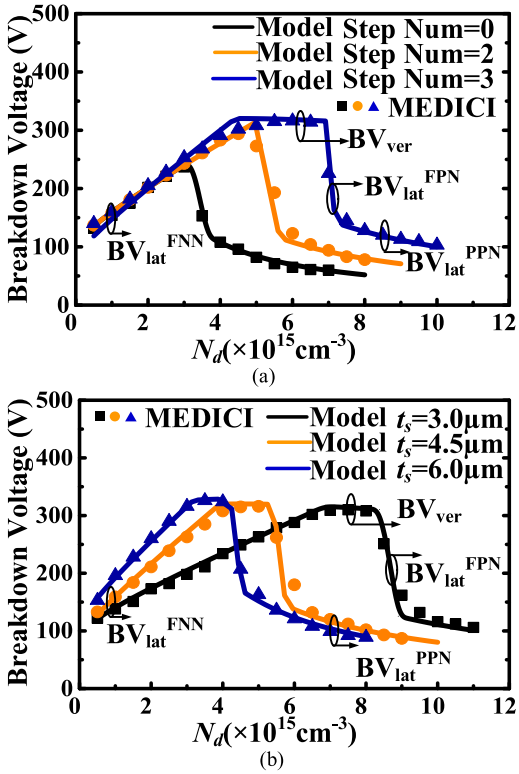

FIGURE 6. The dependence of breakdown voltage on drift region doping under the geometric optimization criterion with various (a) Step number (t_s = 4μm) and (b) Epitaxial layer thickness (Step number=2) with t_{ox} = 2μm, L_d = 20μm.

shown in Fig. 5 (b) and Fig. 6 (a), with the increase of the step number, a more even surface electric field can be achieved. Therefore, the vertical breakdown can be obtained easier allowing a higher actual doping concentration of the drift region. Meanwhile, the epitaxial layer thickness also has a significant effect on the lateral BV characteristic. The thicker epitaxial layer increases the vertical BV yet also causes a stronger step-induced curvature effect. Therefore, as Fig. 6 (b) shows, the vertical breakdown is easier to occur with a smaller t_s. It can be seen in Fig. 6 (b) that with the decrease of the epitaxial layer thickness, both the range and maximum value of actual doping concentration to achieve vertical breakdown can be improved.

V. CONCLUSION

In order to elaborate on the physical meaning of the Stepped drift region thickness technique and its sophisticated effects, we proposed a 1-D methodology to simplify the complicated 2-D problem using the ECP concept. The proposed ST-ECP concept indicates that the influence of the stepped thickness, 2-D RESURF effect, and step-induced curvature effect can be easily obtained by using the principle of compensation semiconductor. Therefore, the inherent 2-D ST device can be equivalent to a 1-D planer junction with ECP when exploring its off-state characteristic. Using the proposed ST-ECP concept, a novel analytical model is proposed to qualitatively and

quantitatively explore the sensitivity of the surface electric field and breakdown voltage to structure parameters for the first time. Based on the proposed model, an effective geometric optimization criterion is proposed to provide designing guidance. The results obtained by the proposed model both are found to be sufficiently accurate as compared to TCAD simulation results.

REFERENCES

[1] D. Disney, T. Letavic, T. Trajkovic, T. Terashima, and A. Nakagawa, "High-voltage integrated circuits: History, state of the art, and future prospects," *IEEE Trans. Electron Devices*, vol. 64, no. 3, pp. 659–673, Mar. 2017, doi: 10.1109/TED.2016.2631125.

[2] X. R. Luo *et al.*, "Ultralow ON-resistance high-voltage p-channel LDMOS with an accumulation-effect extended gate," *IEEE Trans. Electron Devices*, vol. 63, no. 6, pp. 2614–2619, Jun. 2016, doi: 10.1109/TED.2016.2555327.

[3] F. Udrea, G. Deboy, and T. Fujihira, "Superjunction power devices, history, development, and future prospects," *IEEE Trans. Electron Devices*, vol. 64, no. 3, pp. 720–734, Mar. 2017, doi: 10.1109/TED.2017.2658344.

[4] J. Zhang *et al.*, "A new physical insight for the 3-D-layout-induced cylindrical breakdown in lateral power devices on SOI substrate," *IEEE Trans. Electron Devices*, vol. 65, no. 5, pp. 1843–1848, May 2018, doi: 10.1109/TED.2018.2810325.

[5] M. Imam, M. Quddus, J. Adams, and Z. Hossain, "Efficacy of charge sharing in reshaping the surface electric field in high voltage lateral RESURF devices," *IEEE Trans. Electron Devices*, vol. 51, no. 1, pp. 141–148, Jan. 2004, doi: 10.1109/TED.2003.82138.

[6] J. Yao *et al.*, "Analytical model for silicon-on-insulator lateral high-voltage devices using variation of lateral thickness technique," *Jpn J. Appl. Phys.*, vol. 54, no. 2, 2015, Art. no. 024301, doi: 10.7567/JJAP.54.024301.

[7] A. Ferrara, B. K. Boksteen, R. J. E. Hueting, A. Heringa, J. Schmitz, and P. G. Steeneken, "Ideal RESURF geometries," *IEEE Trans. Electron Devices*, vol. 62, no. 10, pp. 3341–3347, Oct. 2015, doi: 10.1109/TED.2015.2460112.

[8] Y. Guo, Z. Wang, and G. Sheu, "Variation of lateral thickness techniques in SOI lateral high voltage transistors," in *Proc. Int. Conf. Commun. Circuits Syst.*, Milpitas, CA, USA, 2009, pp. 611–613, doi: 10.1109/ICCCAS.2009.5250456.

[9] X. Luo, B. Zhang, Z. Li, W. Zhang, Z. Zhan, and H. Xu, "SOI high-voltage device with step thickness sustained voltage layer," *Electron. Lett.*, vol. 44, no. 1, pp. 55–56, Jan. 2008, doi: 10.1049/el:20082131.

[10] Y. Hu *et al.*, "A high-voltage (>600 V) N-island LDMOS with step-doped drift region in partial SOI technology," *IEEE Trans. Electron Devices*, vol. 63, no. 5, pp. 1969–1976, May 2016, doi: 10.1109/TED.2015.2487345.

[11] K. Yang *et al.*, "A novel variation of lateral doping technique in SOI LDMOS with circular layout," *IEEE Trans. Electron Devices*, vol. 65, no. 4, pp. 1447–1452, Apr. 2018, doi: 10.1109/TED.2018.2808193.

[12] J. Zhang, Y.-F. Guo, D. Z. Pan, and F.-R. Hu, "A new physical understanding of lateral step doping technique via effective concentration profile concept," *IEEE Trans. Electron Devices*, vol. 66, no. 5, pp. 2353–2358, May 2019, doi: 10.1109/TED.2019.2903346.

[13] B. J. Baliga and S. K. Ghandhi, "Analytical solutions for the breakdown voltage of abrupt cylindrical and spherical junctions," *Solid-State Electron.*, vol. 19, no. 9, pp. 739–744, 1976, doi: 10.1016/0038-1101(76)90152-0.